Astrocytic tumour grading: a comparative study of three-dimensional pseudocontinuous arterial spin labelling, dynamic susceptibility contrast-enhanced perfusion-weighted imaging, and diffusion-weighted imaging

Hua-Feng Xiao[1] · Zhi-Ye Chen[2] · Xin Lou[2,5] · Yu-Lin Wang[2] · Qiu-Ping Gui[3] ·
Yan Wang[2] · Kai-Ning Shi[4] · Zhen-Yu Zhou[4] · Dan-Dan Zheng[4] · Danny J. J. Wang[5] ·
Lin Ma[2]

Abstract

Objectives We hypothesized that three-dimensional pseudo-continuous arterial spin labelling (pCASL) may have similar efficacy in astrocytic tumour grading as dynamic susceptibility contrast-enhanced perfusion-weighted imaging (DSC-PWI), and the grading accuracy may be further improved when combined with apparent diffusion coefficient (ADC) values.

Methods Forty-three patients with astrocytic tumours were studied using diffusion weighted imaging (DWI), pCASL, and DSC-PWI. Histograms of ADC and normalized tumour cerebral blood flow values (nCBF on pCASL and nrCBF on DSC-PWI) were measured and analyzed.

Results The mean 10 % ADC value was the DWI parameter that provided the best differentiation between low-grade astrocytoma (LGA) and high-grade astrocytoma (HGA). The nCBF and nrCBF (1.810±0.979 and 2.070±1.048) in LGA were significantly lower than those (4.505±2.270 and 5.922±

2.630) in HGA. For differentiation between LGA and HGA, the cutoff values of 0.764×10^{-3} mm^2/s for mean 10 % ADC, 2.374 for nCBF, and 3.464 for nrCBF provided the optimal accuracy (74.4 %, 86.1 %, and 88.6 %, respectively). Combining the ADC values with nCBF or nrCBF could further improve the grading accuracy to 97.7 % or 95.3 %, respectively.

Conclusions pCASL is an alternative to DSC-PWI for astrocytic tumour grading. The combination of DWI and contrast-free pCASL offers a valuable choice in patients with risk factors.

Key Points

• *pCASL shows positive correlation with DSC-PWI in astrocytic tumour grading.*

• *ADC values based on ADC histograms can be an objective method.*

• *Combination of DWI and pCASL or DSC-PWI can improve grading accuracy.*

✉ Xin Lou
louxin301@gmail.com

✉ Lin Ma
cjr.malin@vip.163.com

[1] Department of Radiology, 302 Hospital of Chinese People's Liberation Army, Beijing 100039, China

[2] Department of Radiology, People's Liberation Army General Hospital, No. 28 Fuxing Road, Beijing 100853, China

[3] Department of Pathology, People's Liberation Army General Hospital, Beijing, China

[4] General Electric Healthcare (China) Co., Ltd., Beijing, China

[5] Department of Neurology, University of California, Los Angeles, CA, USA

Abbreviations

HGA	high-grade astrocytoma
LGA	low-grade astrocytoma
nCBF	normalized lesion/normal tissue CBF
nrCBF	normalized lesion/normal tissue rCBF
pCASL	pseudocontinuous arterial spin labelling
rCBF	relative CBF
ROC	receiver operating characteristic

Introduction

Astrocytic tumours of the central nervous system are classified by the World Health Organization into four grades according to pathological appearance. The tumour grading is of great importance in predicting the biological behaviour of the tumours and offers important guidance for accurate tumour biopsy and therapeutic decisions such as surgery, adjuvant radiation, and chemotherapy protocols [1], especially in non-resectable tumours. For these reasons, numerous efforts have been made to assess the astrocytic tumour grading using noninvasive imaging methods. Currently, conventional magnetic resonance imaging (MRI) techniques using T2-weighted image (T2WI), fluid attenuated inversion recovery (FLAIR), and pre-contrast and post-contrast T1-weighted image (T1WI) scans are routinely used for the examination of brain tumours, but accurate assessment of tumour grading cannot be achieved in some cases.

Some of the advanced MRI techniques, such as diffusion weighted imaging (DWI) and dynamic susceptibility contrast-enhanced perfusion-weighted imaging (DSC-PWI), have shown promise in brain tumour grading [1–4]. By providing information derived from the microscopic motion of water molecules, the minimum apparent diffusion coefficient (ADC) values obtained by manually drawn regions of interest (ROIs) on an ADC map can enable the assessment of tumour cellularity and proliferation [4]. Accordingly, minimum ADC values can be used for brain tumour grading. DSC-PWI has been widely used as a valuable method for brain tumour grading, since it can be used to assess the tumour neovascularity. A previous DSC-PWI study suggested that the maximum relative cerebral blood volume (rCBV) and relative cerebral blood flow (rCBF) correlated well with the brain tumour grades [5]. But the application of DSC-PWI involved the use of contrast media injection, which could cause complications, including nephrogenic systemic fibrosis in patients with chronic kidney disease. Arterial spin labelling (ASL) technique, however, is an entirely noninvasive alternative to DSC-PWI, and it could be categorized as either a continuous or pulsed ASL technique [6]. A newly developed ASL sequence, three-dimensional pseudocontinuous arterial spin labelling (pCASL), has potentially combined the advantages of pulsed ASL and continuous ASL, and has attracted significant attention [2, 7–9].

In the present study, ADC values were assessed using an ADC histogram to avoid the possible bias arising from the manual selection of ROIs from the ADC map. Meanwhile, cerebral blood flow (CBF) using pCASL, and rCBF using DSC-PWI were also investigated. The accuracy of brain tumour grading by each technique, as well as the combination of ADC values and contrast-free pCASL sequences, was investigated in a cohort of patients with astrocytic tumours.

Materials and methods

Subjects

This prospective study was approved by institutional ethics committee, and written informed consent was obtained from all the adult patients or from the parents of the paediatric patients. Between May 2012 and September 2014, 43 consecutive patients with suspected astrocytic tumours and preoperative MR imaging examinations including conventional MRI, DWI, pCASL, and DSC-PWI were included in the study. There were 25 males and 18 females, and their age ranged from 6 to 74 years, with a mean age of 43.3 years. All patients received preoperative assessment of internal carotid arteries using MR angiography and there were no significant stenoses. Laboratory tests showed normal renal function in all patients.

MR imaging protocols

All MR images were obtained on a 3.0 T MR scanner (Discovery 750, GE Healthcare, Milwaukee, WI, USA) with a 32-channel head coil. Conventional MR scans included pre-contrast axial T1WI, axial, sagittal, and coronal T2WI, and post-contrast T1WI. T1WI was performed using T1-FLAIR (repetition time/echo time/inversion time [TR/TE/TI] =1, 750 ms/24 ms/780 ms, slice thickness=5.0 mm, slice gap= 1.5 mm, field of view=24×18 cm, matrix=320×320, and NEX=1.0). Axial T2WI was performed using FRFSE (fast recovery fast spin echo) (TR/TE=4,526 ms/111 ms, slice thickness=5.0 mm, slice gap=1.5 mm, field of view=24× 24 cm, matrix=192×192, echo train length=32, and NEX= 1.5). Sagittal and coronal T2WI were performed using T2-FLAIR (TR/TE/TI=8,500 ms/163 ms/2,100 ms, slice thickness=5.0 mm, slice gap=1.5 mm, field of view=20×20 cm, matrix=288×224, and NEX=1.0).

DWI was performed using fat-suppressed single-shot spin-echo echo-planar imaging (TR/TE =6,000 ms/65.7 ms, slice thickness=5.0 mm, slice gap=1.5 mm, field of view=24× 24 cm, matrix=192×192, NEX=2) with b=1,000 s/mm^2 applied in the x, y, and z directions, and b=0 s/mm^2 without motion-probing gradients, followed by automatic generation of isotropic DWI.

pCASL was performed using a background suppressed 3D fast spin echo (FSE) technique. The parameters were as follows: TR=4,653 ms; TE=10.5 ms; post-labelling delay=1, 525 ms; FOV=24×24 cm; matrix=512×512; slice thickness=4.0 mm; slice gap=0 mm; NEX=2, and 36 pairs of tag and control images were acquired in 4 min 30 s. The imaging position extended from the vertex to the base of the skull.

DSC-PWI was then performed with single-shot gradient-recalled echo-planar imaging (GRE-EPI) sequence (TR/TE= 1,525 ms/minimum, 250 Hz/pixel bandwidth for the

acquisition of 20 axial sections, FOV=24×24 cm, 1.0×1.0× 5 mm voxel size, flip angle=60°, matrix=128×128, slice thickness=5 mm, slice gap=1.5 mm, NEX=1, and number of slices=20 for 60 phases). Sixty images were obtained for each slice. Fat saturation was used to optimize the signal-to-noise ratio and baseline values. After five phases, 0.1 mmol/kg Gd-DTPA (Bayer Schering Pharma AG, Berlin, Germany) was injected at a rate of 3 ml/sec, immediately followed by a 20 ml bolus of saline at the same injection rate. The total imaging time was 1 min 32 s. Preload injection of contrast media before DSC-PWI acquisition was not applied.

Post-contrast T1WI was finally performed using FSPGR (fast spoiled gradient recalled echo) (TR/TE/TI=6.2 ms/ 2.8 ms/18 ms, slice thickness=4.0 mm, slice gap=0 mm, field of view=24×24 cm, matrix=288×224) in axial, sagittal, and coronal planes.

MR data processing

ADC, CBF and rCBF color maps were post-processed using Functool software (GE Healthcare, Milwaukee, WI, USA) on a SUN GE AW 4.5 workstation. ADC, CBF, and rCBF measurements were conducted by a neuroradiologist with 5 years' experience in neuroradiology. Patient-related information was removed from all images, and the observer was blinded to the pathological diagnosis. All values were measured again with an interval of 3 months, and the intraobserver agreement was evaluated. The average values of initial and second measurements were regarded as the final ADC, normalized CBF (nCBF), and normalized rCBF (nrCBF) values.

In the present study, an ADC histogram was generated and the parameters involving the entire lesion were used for acquisition. Volume rendering was used to retrieve the ADC map. The tumour volume was obtained in each slice of the axial, coronal, and sagittal planes by identifying the tumour contour with a colored brush and using the histogram pattern to obtain the tumour's ADC histogram. The tumour margins were defined by using conventional T2WI (FRFSE and FLAIR) and post-contrast T1WI, and the necrotic/cystic or hemorrhagic regions in the tumours defined by conventional T2WI, pre-contrast and post-contrast T1WI were avoided in ADC images. By manual placing the metering rod at the lower 10 %, 25 %, and 50 % on ADC histogram curve, the mean 10 %, mean 25 %, mean 50 %, mean, minimum, and maximum ACD values were determined (Figs. 1, 2).

Maximal perfusion values, including maximal CBF (pCASL) and maximal rCBF (DSC-PWI) of the tumours, were measured as follows: on all the continuous pCASL (Figs. 1e, 2e) and DSC-PWI slices (Figs. 1g, 2g), five to eight round ROIs (28–32 mm²) were manually and carefully drawn in the deep color areas within the solid tumour portions on each slice, and the ROIs with the highest CBF and rCBF values were selected from the whole tumour. Those CBF
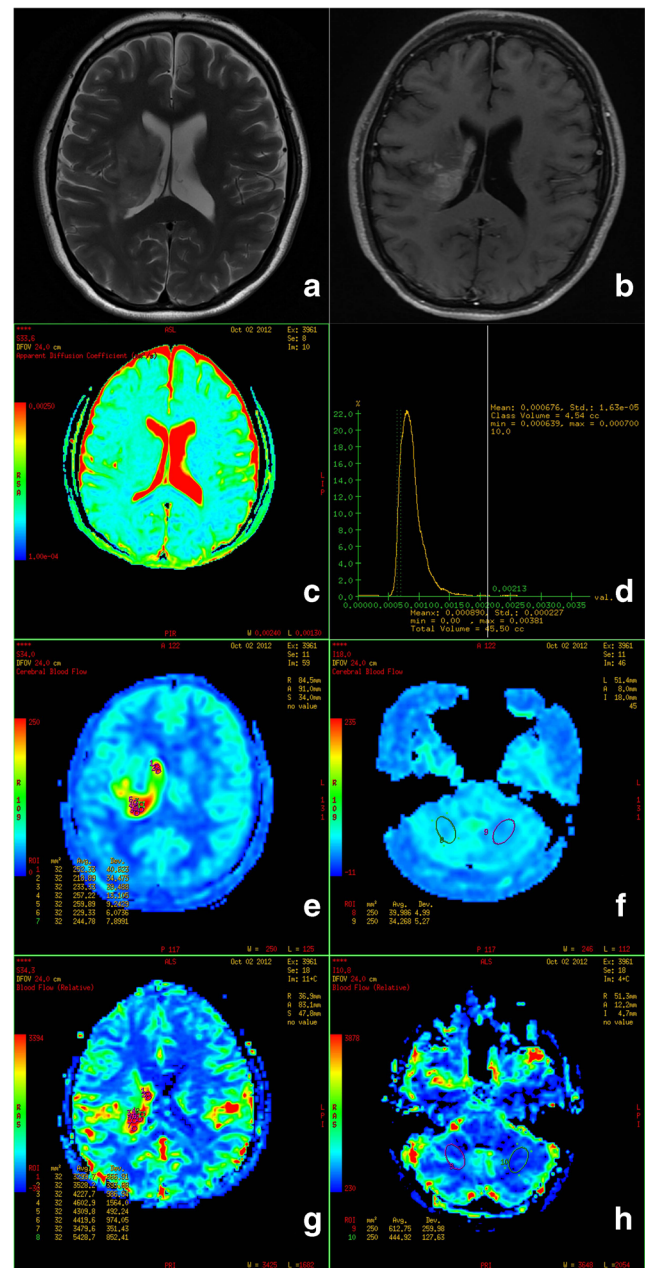

Fig. 1 A sixteen-year-old girl with anaplastic astrocytoma (WHO III) in the right basal ganglion and thalamus. *a* The tumour showed hyperintense signal on T2WI. *b* The tumour showed patchy enhancement on post-contrast T1WI. *c* ADC map. *d* ADC histogram of the tumour. *e* ROI selection for the maximal CBF of the tumour on pCASL CBF color map. *f* ROI selection for bilateral cerebellum CBF on pCASL CBF color map. *g* ROI selection for the maximal rCBF of the tumour on DSC-PWI rCBF color map. *h* ROI selection for bilateral cerebellum rCBF on DSC-PWI rCBF color map

and rCBF values were regarded as the final maximal values. Since some DSC-PWI and PET studies have verified that cerebellar perfusion is usually stable and unaffected by pathology [8, 10, 11], the normalization with the cerebellum was used in the present study, and nCBF on pCASL and nrCBF on DSC-PWI were defined as the mean value for ROI in a tumour area
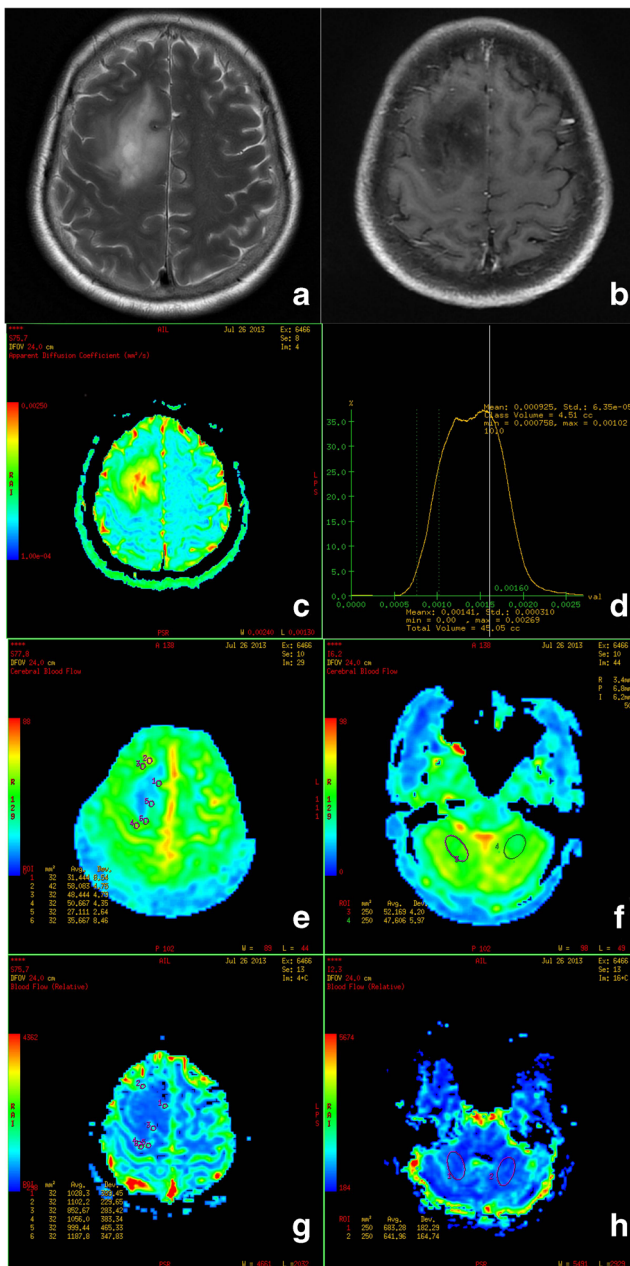
Fig. 2 A sixty-year-old woman with diffuse astrocytoma (WHO II) in the right frontal lobe. *a* The tumour showed hyperintense signal on T2WI. *b* The tumour demonstrated no enhancement on post-contrast T1WI. *c* ADC map. *d* ADC histogram of the tumour. *e* ROI selection for the maximal CBF of the tumour on pCASL CBF color map. *f* ROI selection for bilateral cerebellum CBF on pCASL CBF color map. *g* ROI selection for the maximal rCBF of the tumour on DSC-PWI rCBF color map. *h* ROI selection for bilateral cerebellum rCBF on DSC-PWI rCBF color map

with maximal perfusion/mean value for ROI in cerebellum. Cerebellar ROIs (approximately 250 mm² on each side) were placed in the central regions of the bilateral cerebellar hemispheres (Figs. 1–2f, h), and the mean value was regarded as the reference. Cerebellar reference ROIs were not influenced by cerebellar tumours (one pilocytic astrocytoma) in this study because of the small tumour size.

Pathological observation

All patients underwent navigation-guided (n=28) or open surgery (n=15) within 7 days after the MR scan. For both surgical approaches, the tumour portions with maximal perfusion on MR imaging were used for guidance and should be included in the surgical resection. All specimens obtained for pathological observation were fixed in formalin and embedded in paraffin. Hematoxylin and eosin-stained and immunohistochemically prepared specimens were performed to determine the histological type of the tumour after surgery. The pathological diagnosis was made by a pathologist with 20 years of experience in neuropathology. According to the World Health Organization (WHO) criteria [12], tumours of WHO grade I and II were classified as low-grade astrocytoma (LGA), whereas tumours of WHO grade III and IV were classified as high-grade astrocytoma (HGA).

Statistical analysis

Intraobserver agreement was assessed with the intraclass correlation coefficient (ICC), in which ICC<0.40=poor, 0.40–0.59=fair, 0.60–0.74=good, and>0.74=excellent.

All statistical analyses were performed using the statistical package SPSS for Windows (Version 16.0, Chicago, IL, USA). The level of significance was set at $p<0.05$. ADC values, nCBF and nrCBF between LGA and HGA were analyzed and compared using one-way ANOVA and Student's unpaired t-test.

Pearson's correlation analysis was performed between nCBF and nrCBF, between ADC values and nCBF, and between ADC values and nrCBF, respectively.

Receiver operating characteristic (ROC) curves for ADC values, nCBF, and nrCBF were applied to assess the cutoff value that best balanced sensitivity and specificity to allow differentiation between LGA and HGA. Binary logistic regression was performed using mean 10 % ADC + nCBF, and mean 10 % ADC + nrCBF, respectively. In each patient, five predicted probabilities produced from mean 10 % ADC, nCBF, nrCBF, mean 10 % ADC + nCBF, and mean 10 % ADC + nrCBF were set as the variables, and each predicted probability was evaluated using ROC curve [13].

Results

Pathological results

Nineteen LGAs (one pilocytic astrocytoma and 18 diffuse astrocytomas) and 24 HGAs (six anaplastic astrocytomas and 18 glioblastomas) were proved by pathology.

ICC evaluation

The intraobserver reproducibility of mean 10 % ADC measurements on ADC histogram, nCBF measurements on 3D-pCASL, and nrCBF measurements on DSC-PWI was excellent. ICCs were 0.927 for ADC values, 0.869 for nCBF, and 0.850 for nrCBF, respectively.

ADC histogram parameters, nCBF, and nrCBF

The ADC values of LGA were significantly higher than those of HGA using the mean 10 %, mean 25 %, mean, and minimum ADC values, and the difference was most significant by using the mean 10 % ADC value ($p<0.001$). The differences were not significant using the mean 50 % and maximum ADC values (Table 1).

The nCBF (1.810 ± 0.979) in the LGA group was significantly lower than that (4.505 ± 2.270) in the HGA group ($p<0.001$), and the nrCBF (2.070 ± 1.048) in the LGA group was significantly lower than that (5.922 ± 2.630) in the HGA group ($p<0.001$) (Table 2).

Pearson's correlation analysis showed a significant positive correlation between nCBF and nrCBF ($r=0.751$, $p<0.001$) (Fig. 3a). The mean 10 % ADC value was chosen, and Pearson's correlation analysis showed a negative correlation between the mean 10 % ADC and nCBF ($r=-0.323$, $p<0.01$) (Fig. 3b) and between mean 10 % ADC and nrCBF ($r=-0.430$, $p<0.01$) (Fig. 3c).

ROC analysis

The results of the ROC analysis using the mean 10 % ADC value, nCBF, nrCBF, mean 10 % ADC + nCBF, and mean 10 % ADC + nrCBF for the differentiation between LGA and HGA were presented in Table 3 and Fig. 4. The accuracy was 74.4 % for mean 10 % ADC value, 86.1 % for nCBF, and 88.6 % for nrCBF, respectively. Combining the cutoff value of mean 10 % ADC with nCBF or nrCBF could improve the grading accuracy up to 97.7 % or 95.3 %, respectively.

Table 1 ADC histogram values (mean±SD) ($\times10^{-3}$ mm^2/s) of LGA and HGA

	LGA ($n=19$)	HGA ($n=24$)	p value
Mean 10 % ADC	0.886±0.118	0.745±0.079	< 0.001
Mean 25 % ADC	1.005±0.195	0.844±0.089	0.003
Mean 50 % ADC	1.167±0.302	1.239±0.108	0.752
Mean ADC	1.418±0.375	1.204±0.188	0.019
Minimum ADC	0.625±0.071	0.548±0.093	0.038
Maximum ADC	3.437±0.578	3.310±0.676	0.519

SD=standard deviation

Table 2 The nCBF and nrCBF (mean±SD) of LGAs and HGAs

	LGA (n=19)	HGA (n=24)	p value
nCBF	1.810±0.979	4.505±2.270	< 0.001
nrCBF	2.070±1.048	5.922±2.630	< 0.001

SD=standard deviation

According to the linear interpolation method, the diagnostic point based on the ROC was calculated as predicted probability for mean 10 % ADC + nCBF (P1) or predicted probability for mean 10 % ADC + nrCBF (P2). The best diagnostic points were 0.354 for P1 and 0.488 for P2, respectively, which meant if the predicted probability was higher than or equal to 0.354 or 0.488, the tumour could be diagnosed as HGA rather than LGA, and vice versa. The logistic regression equation was built and is described as follows:

$$P1 = \frac{1}{1 + e^{-(15.544 - 2.657E4X1 + 2.445X2)}}$$

$$P2 = \frac{1}{1 + e^{-(19.758 - 3.027E4X1 + 1.371X3)}}$$

(X$_1$: mean 10 % ADC value; X$_2$: nCBF value; X$_3$: nrCBF value; E4: 10^4)

Discussion

In this study, we noted that a close correlation was presented between nCBF (3D-pCASL) and nrCBF (DSC-PWI) in astrocytic tumour grading, which was in agreement with the results of previous studies [14]. Although the overlap in nCBF or nrCBF at the cutoff values was noticed, most patients in the LGA group had values below the threshold, while most patients in the HGA group had values above the threshold. One grade II astrocytoma, which abutted the cerebral convexity and falx, showed obvious hyperperfusion on 3D-pCASL with an increased nCBF value of 4.88. The possible explanation could be that the tumour was closely related with the adjacent meningeal vessels. However, its nrCBF value of 1.58 was not as high as expected. Susceptibility of DSC-PWI may result in decreased perfusion in such superficial lesions.

A histogram is a plot in which widths represent class intervals and areas are proportional to the corresponding frequencies. The key point was to ensure that the tumour boundary should be outlined accurately by encompassing the entire tumour, avoiding necrosis, haemorrhage, and peripheral oedema. Although multiple parameters from the ADC histogram can be used to grade astrocytic tumours, the statistical results indicated that in this study the mean 10 % ADC value was most significant in differentiating LGA from HGA. The cutoff value of mean 10 % ADC (0.764×10^{-3} mm^2/s) in this study was
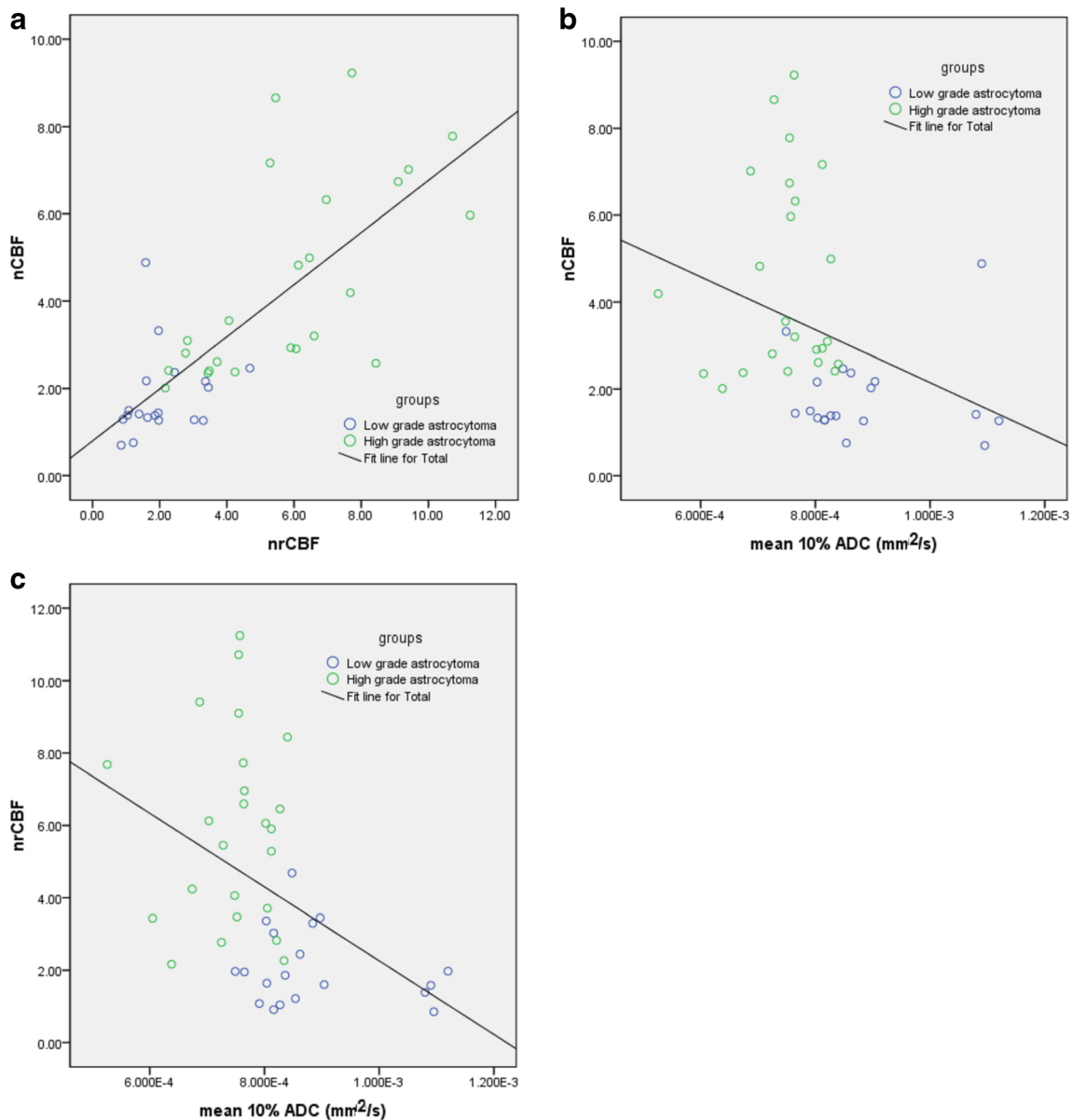
Fig. 3 *a* Scatterplot of the correlation between the nCBF and nrCBF in LGAs and HGAs. *b* Scatterplot of the correlation between the mean 10 % ADC value and nCBF in LGAs and HGAs. *c* Scatterplot of the correlation between the mean 10 % ADC value and the nrCBF in LGAs and HGAs

lower than those (0.900×10^{-3} mm^2/s and 1.01×10^{-3} mm^2/s) reported in other studies based on manual ROI measurement [4, 15]. The discrepancy might be mainly due to the differences in the sampling methodology. Moreover, disruptions in the

Table 3 ROC analysis of the mean 10 % ADC ($\times 10^{-3}$ mm2/s), nCBF, nrCBF, mean 10 % ADC+ nCBF, and mean 10 % ADC+ nrCBF values for astrocytic tumour grading

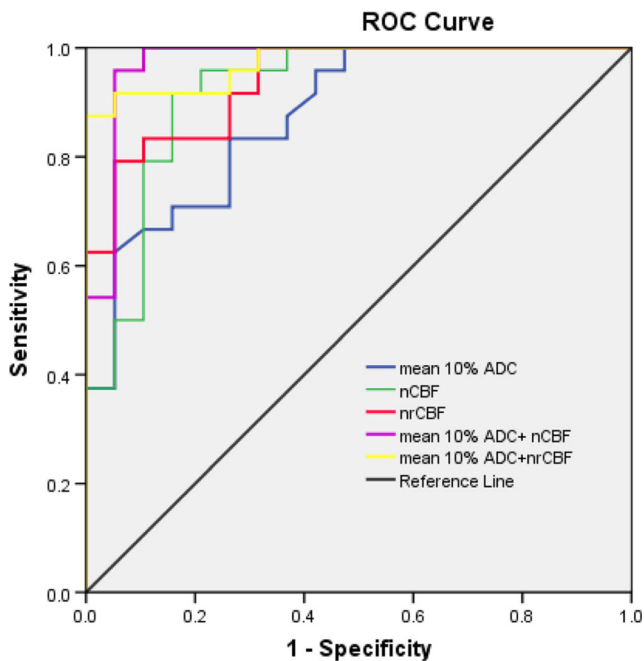|	Cutoff value	AUC	Sensitivity	Specificity	Accuracy
Mean 10 % ADC	0.764	0.875	94.7 %	62.5 %	74.4 %
nCBF	2.374	0.919	91.7 %	84.2 %	86.1 %
nrCBF	3.464	0.939	79.2 %	94.7 %	88.6 %
Mean 10 % ADC + nCBF	N/A	0.974	N/A	N/A	97.7 %
Mean 10 % ADC + nrCBF	N/A	0.974	N/A	N/A	95.3 %

N/A=not available

Fig. 4 ROC map of the mean 10 % ADC, nCBF, nrCBF, mean 10 % ADC+ nCBF, and mean 10 % ADC+ nrCBF values for the discrimination of LGAs vs. HGAs

class intervals on histogram were found in some tumours, which could be compensated by using the mean 10 % ADC value. Future study is needed to compare the accuracy between histogram-generated ADC values and manual ROI-defined ADC values in tumour grading [4, 15, 16].

The present investigation demonstrated that an inverse correlation existed between mean 10 % ADC value and both nCBF and nrCBF, suggesting that increased cellularity (low ADC) was correlated with high vascularity (high nCBF or nrCBF) in astrocytic tumours. ADC value could be used in astrocytic tumour grading, which has been shown to reflect the histologically determined cellular density [17, 18]. We believe that mean 10 % ADC value had intrinsic advantages, although its overall efficacy was inferior to pCASL and DSC-PWI in this study. For example, the ADC value could be used to compensate for the decreased grading accuracy in some LGAs with high CBF or HGAs with low CBF. One aforementioned case of grade II astrocytoma with hyperperfusion on nCBF could be properly graded as LGA by using the mean 10 % ADC value (0.848×10^{-3} mm^2/s), which was higher than the cutoff value (0.764×10^{-3} mm^2/s)[19]. In this case, a correct tumour grading could also be achieved by using *P2* value (0.023), which was lower than the diagnostic point (0.488).

In this study, the accuracy for astrocytic tumour grading was improved by combining the mean 10 % ADC value with perfusion-base techniques such as 3D-pCASL or DSC-PWI as compared with individual methods. Our results also indicated that the accuracy of astrocytic tumour grading by combined ADC value and perfusion parameters was higher than

those in previous studies [1, 10, 15, 20]. The authors considered that the use of predicted probabilities (P1 and P2 values) was practicable in clinical practice. Moreover, when the patients were under the conditions of chronic kidney disease, dialysis, hyperphosphatemia, acidosis, and pro-inflammatory events, gadolinium-based contrast agents should be used with caution [21], and the combination of MR techniques, including ADC values and contrast-free pCASL, should be the preferred method of choice for tumour grading.

Limitations of the present study were as follows. 1) The sample size was not large enough to make a further discussion on histological subtypes of LGAs and HGAs. 2) Only one post-labelling delay time (1,525 ms) in pCASL was used, which may have potential influences on the evaluation of cerebral flow in some cases. 3) Uncorrected maps in pCASL were used. To decrease the partial volume effects of pCASL acquisitions, a previous study acquired both uncorrected maps and maps corrected for partial volume effects, which yielded similar results, and CBF maps corrected for partial volume effects were not feasible for clinical use [22]. 4) Different slice thickness existed between 3D pCASL and 2D DSC-PWI; therefore, voxel-wise correlation could not be achieved between them, but anatomical correlation could be determined in assessing the perfusion values. 5) A major concern about the calculation errors of nrCBF values with DSC-PWI is the leakage of contrast agent from the vasculature to the tumour. Attempts to correct the calculation errors include preload injection of a small amount of contrast agent, use of dual-echo pulse sequence and baseline subtraction, but none of them are considered to be the satisfactory method of choice. Therefore, DSC-PWI without preload of contrast agent are clinically acceptable.

In conclusion, the mean 10 % ADC value based on ADC histogram had its intrinsic advantages and could be an objective method in predicting astrocytic tumour grading. pCASL could be reliably applied in tumour grading, since it had a significant positive correlation with DSC-PWI. The combination of ADC values and pCASL or DSC-PWI could markedly improve the accuracy for astrocytic tumour grading. Particularly, the combination of ADC values and contrast-free pCASL sequences could offer a clinically valuable method of choice in patients with major risk factors and in patients who need follow-up studies.

References

1. Law M, Yang S, Wang H et al (2003) Glioma grading: sensitivity, specificity, and predictive values of perfusion MR imaging and proton MR spectroscopic imaging compared with conventional MR imaging. AJNR Am J Neuroradiol 24:1989–1998

2. Roy B, Awasthi R, Bindal A et al (2013) Comparative evaluation of 3-dimensional pseudocontinuous arterial spin labeling with dynamic contrast-enhanced perfusion magnetic resonance imaging in grading of human glioma. J Comput Assist Tomogr 37:321–326

3. Romano A, Rossi Espagnet MC, Calabria LF et al (2012) Clinical applications of dynamic susceptibility contrast perfusion-weighted MR imaging in brain tumours. Radiol Med 117:445–460

4. Chen Z, Ma L, Lou X et al (2010) Diagnostic value of minimum apparent diffusion coefficient values in prediction of neuroepithelial tumor grading. J Magn Reson Imaging 31:1331–1338

5. Barrett T, Brechbiel M, Bernardo M et al (2007) MRI of tumor angiogenesis. J Magn Reson Imaging 26:235–249

6. Petcharunpaisan S, Ramalho J, Castillo M (2010) Arterial spin labeling in neuroimaging. World J Radiol 2:384–398

7. Nielsen JF, Hernandez-Garcia L (2013) Functional perfusion imaging using pseudocontinuous arterial spin labeling with low-flip-angle segmented 3D spiral readouts. Magn Reson Med 69:382–390

8. Jarnum H, Steffensen EG, Knutsson L et al (2010) Perfusion MRI of brain tumours: a comparative study of pseudo-continuous arterial spin labelling and dynamic susceptibility contrast imaging. Neuroradiology 52:307–317

9. Wheaton AJ, Miyazaki M (2012) Non-contrast enhanced MR angiography: physical principles. J Magn Reson Imaging 36:286–304

10. Thomsen H, Steffensen E, Larsson EM (2012) Perfusion MRI (dynamic susceptibility contrast imaging) with different measurement approaches for the evaluation of blood flow and blood volume in human gliomas. Acta Radiol 53:95–101

11. Arbab AS, Aoki S, Toyama K et al (2001) Brain perfusion measured by flow-sensitive alternating inversion recovery (FAIR) and dynamic susceptibility contrast-enhanced magnetic resonance imaging: comparison with nuclear medicine technique. Eur Radiol 11:635–641

12. Fuller GN, Scheithauer BW (2007) The 2007 Revised World Health Organization (WHO) Classification of Tumours of the Central Nervous System: newly codified entities. Brain Pathol 17:304–307

13. Chen Z, Feng F, Yang Y et al (2012) MR imaging findings of the corpus callosum region in the differentiation between multiple sclerosis and neuromyelitis optica. Eur J Radiol 81:3491–3495

14. Lehmann P, Monet P, de Marco G et al (2010) A comparative study of perfusion measurement in brain tumours at 3 Tesla MR: arterial spin labeling versus dynamic susceptibility contrast-enhanced MRI. Eur Neurol 64:21–26

15. Murakami R, Hirai T, Sugahara T et al (2009) Grading astrocytic tumors by using apparent diffusion coefficient parameters: superiority of a one- versus two-parameter pilot method. Radiology 251:838–845

16. Bilgili Y, Unal B (2004) Effect of region of interest on interobserver variance in apparent diffusion coefficient measures. AJNR Am J Neuroradiol 25:108–111

17. Gupta RK, Cloughesy TF, Sinha U et al (2000) Relationships between choline magnetic resonance spectroscopy, apparent diffusion coefficient and quantitative histopathology in human glioma. J Neurooncol 50:215–226

18. Rollin N, Guyotat J, Streichenberger N et al (2006) Clinical relevance of diffusion and perfusion magnetic resonance imaging in assessing intra-axial brain tumors. Neuroradiology 48:150–159

19. Rumboldt Z, Camacho DL, Lake D et al (2006) Apparent diffusion coefficients for differentiation of cerebellar tumors in children. AJNR Am J Neuroradiol 27:1362–1369

20. Kim MJ, Kim HS et al (2008) Diagnostic accuracy and interobserver variability of pulsed arterial spin labeling for glioma grading. Acta Radiol 49:450–457

21. Zou Z, Ma L, Li H (2009) Incidence of nephrogenic systemic fibrosis at Chinese PLA General Hospital. J Magn Reson Imaging 30:1309–1312

22. Binnewijzend MA, Kuijer JP, Benedictus MR et al (2013) Cerebral blood flow measured with 3D pseudocontinuous arterial spin-labeling MR imaging in Alzheimer disease and mild cognitive impairment: a marker for disease severity. Radiology 267:221–230